

ATXN2 Knockout Mitigates TDP-43–Induced Transcriptomic Dysregulation in ALS Motor Neurons

Eddie Ma

Basis Independent Silicon Valley (BISV), 1290 Parkmoor Ave, San Jose, CA 95126, United States

ABSTRACT

Amyotrophic lateral sclerosis (ALS) is a devastating progressive neurodegenerative disorder characterized by the loss of motor neurons in the brain and spinal cord. TDP-43 proteinopathy is a hallmark of nearly all ALS cases. This study reanalyzed transcriptome RNA-seq dataset GSE261875 and characterized transcriptomic changes induced by nuclear overexpression of wild-type TDP-43 (wTDP) and cytoplasmic mislocalization of TDP-43 (cTDP) in human iPSC-derived motor neurons, and ascertained the effects of CRISPR-mediated ATXN2 knockout (AKO) on these cells. PCA plots revealed distinct clusters of wTDP, cTDP and Neg CTRL. DEG analysis between wTDP and Neg CTRL yielded 3,222 up- and 3,302 down-regulated DEGs, while that between cTDP and Neg CTRL identified 2,828 up- and 2,949 down-regulated DEGs. Shared DEGs (964 up, 820 down) between wTDP and cTDP were enriched for ALS-relevant pathways. Further, PCA plots revealed distinct clusters of wTDP-AKO, cTDP-AKO, wTDP, and cTDP. ATXN2 knockout reversed many TDP-43–induced changes, including 2,794 up- and 2,956 down-regulated DEGs between wTDP-AKO and wTDP groups, and 3,024 up- and 2,838 down-regulated DEGs between cTDP-AKO and cTDP groups. Integration of shared DEGs between the two TDP-43–induced and ATXN2-reversed groups defined a core signature list comprising 125 pathogenic and 222 protective genes that may be potential biomarkers to ALS pathogenesis and its attenuation. The identification of both pathogenic and protective gene signatures provides novel molecular insights into ALS pathogenesis and highlights ATXN2 as a promising therapeutic target. These findings not only refine candidate biomarker panels for ALS but also open new ways for targeted therapy.

Keywords: ALS; TDP-43; wild-type; cytoplasmic; ATXN2; pathogenic; protective

INTRODUCTION

Amyotrophic lateral sclerosis (ALS) is a devastating progressive neurodegenerative disorder characterized by the loss of motor neurons in the brain and spinal cord (1). Historically, ALS was considered as a purely motor neuron disease that affects the brain,

spinal cord, and skeletal muscles. However, advances in neurobiology and clinical neuropathology have redefined ALS as a multisystem disorder involving genetics, epigenetics, immune dysregulation, and systemic metabolic changes (1).

In ALS, degenerations of upper motor neurons in the motor cortex and lower motor neurons in the brainstem and spinal cord result in progressive impairment of both voluntary and involuntary motor functions. Clinically, ALS often presents with subtle focal muscle weakness or stiffness, typically starting in the distal extremities. Within a short period of time, symptoms spread to bulbar, axial, and respiratory musculature. Patients

Corresponding author: Eddie Ma, E-mail: EddieMa4700@Gmail.com.

Copyright: © 2026 Eddie Ma. This is an open access article distributed under the terms of the Creative Commons Attribution License, which permits unrestricted use, distribution, and reproduction in any medium, provided the original author and source are credited.

Accepted January 28, 2026

<https://doi.org/10.70251/HYJR2348.41508518>

commonly develop spasticity, cramping, dysarthria, dysphagia, gait disturbance, and eventually complete paralysis (2). Respiratory muscle weakness is the primary cause of mortality (1, 2). The median survival time is approximately 20-48 months from symptom onset (3). Current therapies, including disease slowing medications (riluzole, edaravone, and Relyvrio), gene-targeted approaches (Tofersen), immunomodulation, and experimental stem cell–exosome therapies, seek to slow disease progression and alleviate symptoms, but available options remain limited and largely ineffective (4).

The pathogenesis of ALS is complex and involves dysregulations in protein homeostasis, RNA metabolism, mitochondrial function, glutamate-mediated excitotoxicity, and axonal transport (5). Over 120 genes have been implicated in ALS susceptibility and progression, with TARDBP (TDP-43), C9orf72, SOD1, and FUS among the most significant. Mutations in TARDBP cause dysfunction of TDP-43, a DNA- and RNA-binding protein, whose cytoplasmic aggregation is observed in approximately 97% of ALS cases (6). Under normal conditions, TDP-43 resides in the nucleus, where it regulates transcription, RNA maturation, transport, and stability. In ALS, nuclear TDP-43 becomes hyperphosphorylated and proteolytically cleaved into C-terminal fragments that mislocalize to the cytoplasm, forming inclusions with toxic gain-of-function effects while also resulting in a loss of normal nuclear functions (7). This TDP-43 proteinopathy is a hallmark in almost all ALS patients. Many ALS patients with TDP-43 proteinopathy lack TARDBP mutations, suggesting that multiple upstream mechanisms converge to trigger TDP-43 proteinopathy (i.e. TDP-43 mislocalization and aggregation) (8).

Additionally, disruption of the ubiquitin–proteasome system and autophagy lead to the accumulation of misfolded and aggregated proteins, including TDP-43, SOD1, and FUS (9). Defective RNA splicing, transport, and stability are common in ALS, driven in part by dysfunction of RNA-binding proteins such as TDP-43 and FUS, which also disrupt stress granule dynamics. Mitochondrial abnormalities impair oxidative phosphorylation and promote oxidative stress, while glutamate excitotoxicity, possibly due to decreased expression of the astrocytic glutamate transporter EAAT2, induces calcium overload and neuronal injury. Impaired axonal transport, resulting from cytoskeletal and motor protein dysfunction, further compromises the delivery of essential cargo to and from the neuronal soma, accelerating degeneration (5, 6, 7).

Direct therapeutic targeting of TDP-43 remains challenging, as depletion of TDP-43 in animal models induces ALS-like phenotypes and early lethality (10). Ataxin-2 (ATXN2) is an RNA-binding protein involved in RNA metabolism and stress granule formation. ATXN2 contains a polyglutamine (CAG) repeat tract in its coding sequence, and are associated with increased ALS risk (11). ATXN2 has emerged as a potent genetic modifier of TDP-43 toxicity in yeast, fly, and mouse models. Knockout or suppression of ATXN2 extends survival in TDP-43 transgenic mice and reduces TDP-43–induced toxicity across multiple model systems (11,12). These findings suggest that ATXN2 reduction as a viable therapeutic strategy, but the underlying mechanisms in human motor neurons remain unclear.

To address this gap, this study reanalyzed bulk RNA-seq dataset GSE261875, obtained from human iPSC-derived motor neurons subjected to negative control (Neg CTRL) and two TDP-43 transfected conditions, namely overexpression of nuclear type TDP-43 (wTDP) and cytoplasmic TDP-43 (cTDP). Some of these wTDP and cTDP cells were further subjected to CRISPR-mediated ATXN2 knockout (AKO) (wTDP-AKO and cTDP-AKO). By characterizing transcriptomic changes and pathways relevant to ALS pathogenesis and ATXN2-mediated neuroprotection, this study investigated molecular signatures and mechanisms that could inform the development of biomarkers and targeted therapies for TDP-43 proteinopathies in ALS.

METHODS AND MATERIALS

RNA-Seq Dataset Acquisition and Processing

Bulk RNA-seq data in dataset GSE261875 were downloaded from the NCBI Gene Expression Omnibus (13). These data had been obtained from human motor neurons generated *in vitro* from the 11a induced pluripotent stem cell (iPSC) line derived from a skin biopsy of a healthy 37-year-old male, as previously described (14, 15) In that study, differentiated motor neurons after 7 days induction were then transfected with one of the following constructs for another 5 days culturing: empty vector control (negative control; Neg CTRL; n=4), wild-type TDP-43 (wTDP; n=4), or a cytoplasmically localized TDP-43 variant (cTDP; n=4) lacking the nuclear localization signal, thereby mimicking the pathological cytoplasmic aggregation observed in ALS patients. ATXN2 knockout (AKO) was achieved using CRISPR-mediated gene editing followed by single-cell cloning. The resulting groups were named

as wTDP AKO (n=4) and cTDP AKO (n=4). RNA was harvested after total 12 days in culture for bulk RNA-seq. After data download, the raw sequencing reads from the GSE261875 dataset were quality-trimmed, normalized, and log₂-transformed using R software packages. Five experimental groups were included in the dataset, and four pairwise differential expression (DE) analyses were performed: Neg CTRL vs. wTDP, Neg CTRL vs. cTDP, wTDP-AKO vs. wTDP, and cTDP-AKO vs. cTDP.

Data Analysis

Sequence reads had been mapped to the human reference genome (GRCh38) by the authors who generated the original dataset. Data analyses in this study began with gene-level raw count data. Gene counts were annotated with gene symbols and descriptions, then filtered to remove low-abundance and unannotated genes. The filtered data were normalized and log₂-transformed. Log₂-transformed expression values were used for differential expression and pathway analyses in this study. All data processing and analyses were performed using R packages.

Differential expression analysis was performed by using the edgeR package (version 4.2.0) in R packages. Genes with an absolute log₂ fold change ($|\log_2FC|$) > 0.2 and a false discovery rate (FDR) < 0.05 were considered differentially expressed. Adjusted p-values (padj) for multiple testing, using Benjamini-Hochberg to estimate the false discovery rate (FDR), were calculated for final estimation of DE significance. Gene Ontology (GO) enrichment analysis was performed on significantly differentially expressed genes (DEGs) by using the clusterProfiler package (version 4.12.2) in R. GO terms in

the biological process, cellular component, and molecular function categories were assessed, and considered significantly enriched if both the FDR and the q-value were <0.05. Unsupervised principal component analysis (PCA), volcano plots, heatmaps, and dot plots were generated for visualization of gene expression changes and functional patterns relevant to ALS-associated neurodegeneration.

RESULTS

Distinct Transcriptomic Signatures of human motor neurons induced by TDP-43 variants

PCA showed clear separation among the three groups of cells, namely the empty vector control group (Neg CTRL), those overexpressing wTDP variants, and those expressing cTDP variants (Figure 1A). Similarly, PCA of CRISPR-mediated ATXN2 knockout groups in the context of TDP-43 variants, including wTDP-AKO, cTDP-AKO, and their respective controls, also revealed distinct clustering of these groups of cells (Figure 1B).

Differential Gene Expression in wTDP vs. Neg CTRL

A comparison of Neg CTRL and wTDP groups identified 3,222 up- and 3,302 down-regulated DEGs in wTDP group (Table 1, Figure 2A). GO enrichment analysis revealed that these DEGs were significantly associated with key biological processes (BP), cellular components (CC), and molecular functions (MF) relevant to ALS pathogenesis (Figure 2B–D). These changes in the transcriptional profiles revealed molecular alterations in motor neurons overexpressing the wild-type TDP.

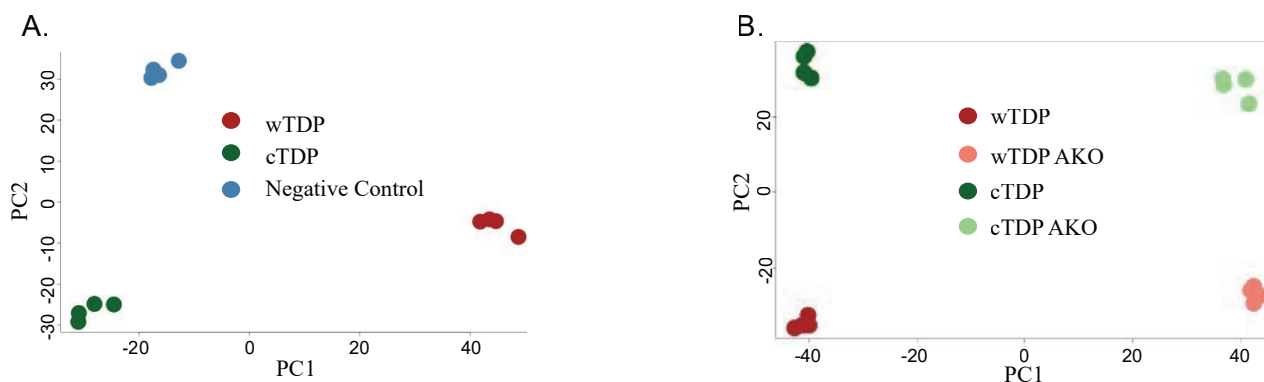


Figure 1. PCA revealed distinct transcriptomic signatures among Neg CTRL motor neurons and those subjected to TDP-43 variants. (A) PCA of wTDP, cTDP and Neg CTRL. (B) PCA of wTDP, wTDP-AKO, cTDP and cTDP AKO.

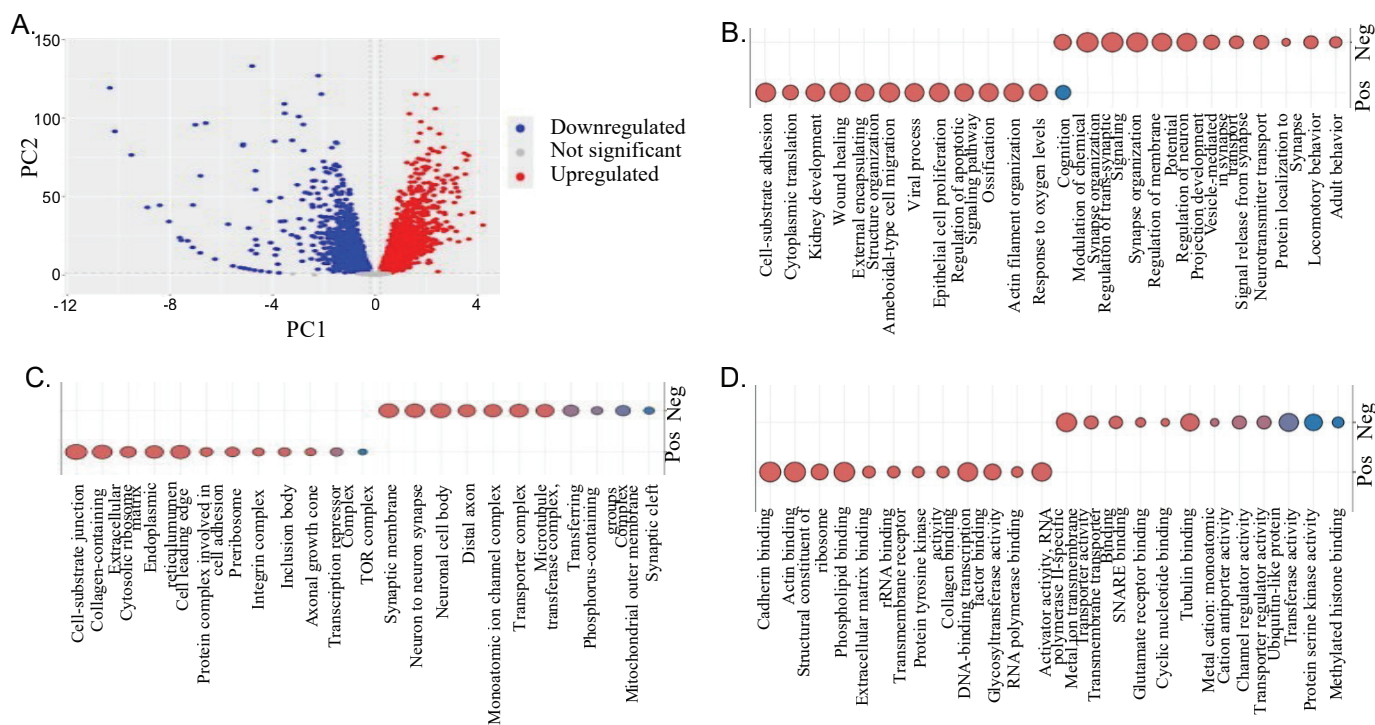


Figure 2. DEGs in a comparison of wTDP vs Neg CTRL. (A) Volcano plot of the DEGs. (B-D) Enriched pathways (BP, CC, and MF) based on GO enrichment analysis of the DEGs.

Differential Gene Expression in cTDP vs. Neg CTRL

A comparison of Neg CTRL and cTDP identified 2,828 up- and 2,949 down-regulated DEGs in cTDP group (Table 1, Figure 3A). Similar to those in wTDP, GO enrichment analysis revealed pathways in ALS-relevant BP, CC, and MF categories (Figure 3B–D). These data indicated that the cTDP condition, which mimics cytoplasmic mislocalization of TDP-43, induced broad transcriptional reprogramming similar to the pathological processes observed in ALS.

Shared DEGs in wTDP and cTDP vs. Neg CTRL

Despite distinct clustering of wTDP and cTDP samples in PCA, a total of 964 upregulated and 820 downregulated genes were shared between wTDP vs.

Neg CTRL and cTDP vs. Neg CTRL (Table 1, Figure 4A–B). GO enrichment analyses (Figure 4C–D) showed convergent dysregulation of pathways associated with neuronal function, protein homeostasis, and RNA metabolism. There were no significant MF enrichment pathways. These genes and pathways indicate the shared genes and pathways between overexpressed nuclear TDP and cytoplasmic TDP mislocalization-induced proteinopathy in ALS.

Neuroprotective Effects of ATXN2 Knockout

Next, the impact of ATXN2 knockout on TDP-43–induced changes was assessed. In a comparison of wTDP-AKO vs. wTDP, 2,794 genes were up- and 2,956 down-regulated (Table 1, Figure 5A). GO enrichment analysis

Table 1. The numbers of DEGs in wTDP and cTDP compared with their Neg CTRL.

Gene Counts	Comparing	Neg CTRL VS wTDP	Neg CTRL VS cTDP	Shared DEGS
	Up-regulated Gene Counts		3222	2828
Down-regulated Gene Counts		3302	2949	820

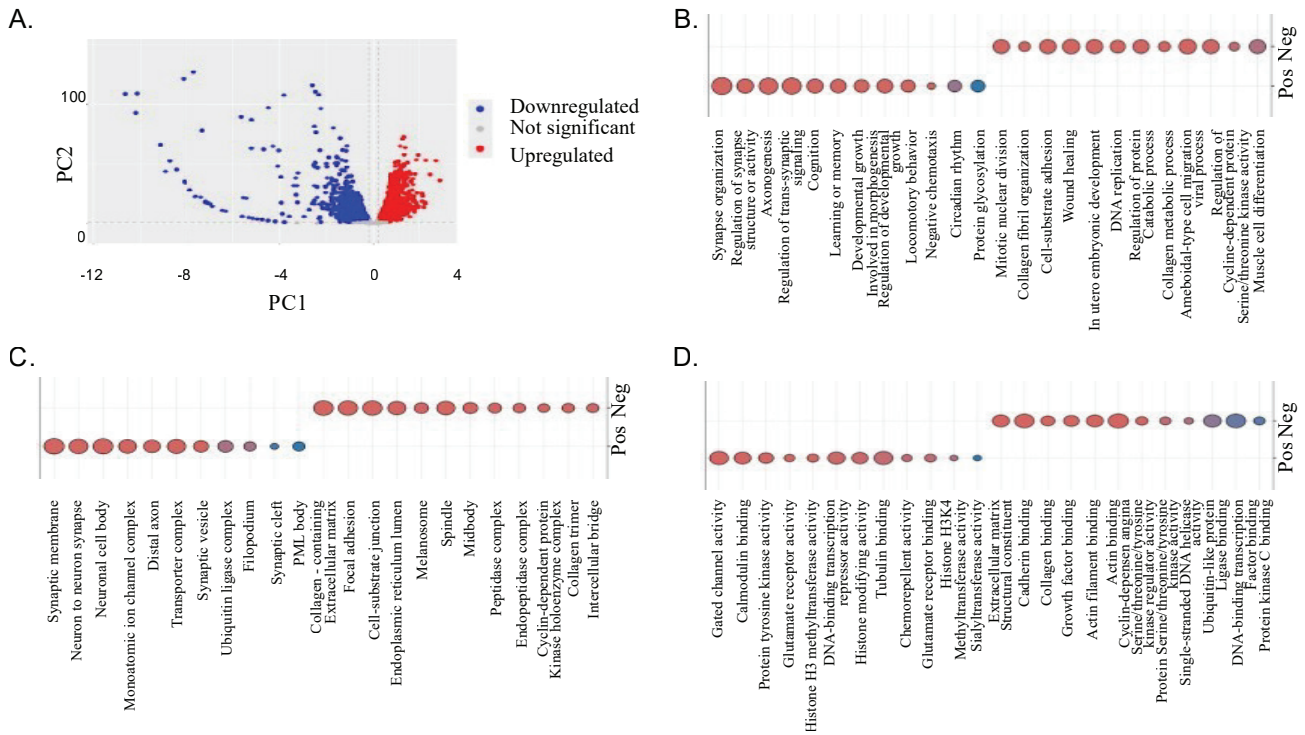


Figure 3. DEGs analysis of cTDP vs Neg CTRL. (A) Volcano plot of the DEGs. (B-D) Enriched pathways (BP, CC, and MF) based on GO enrichment analysis of DEGs.

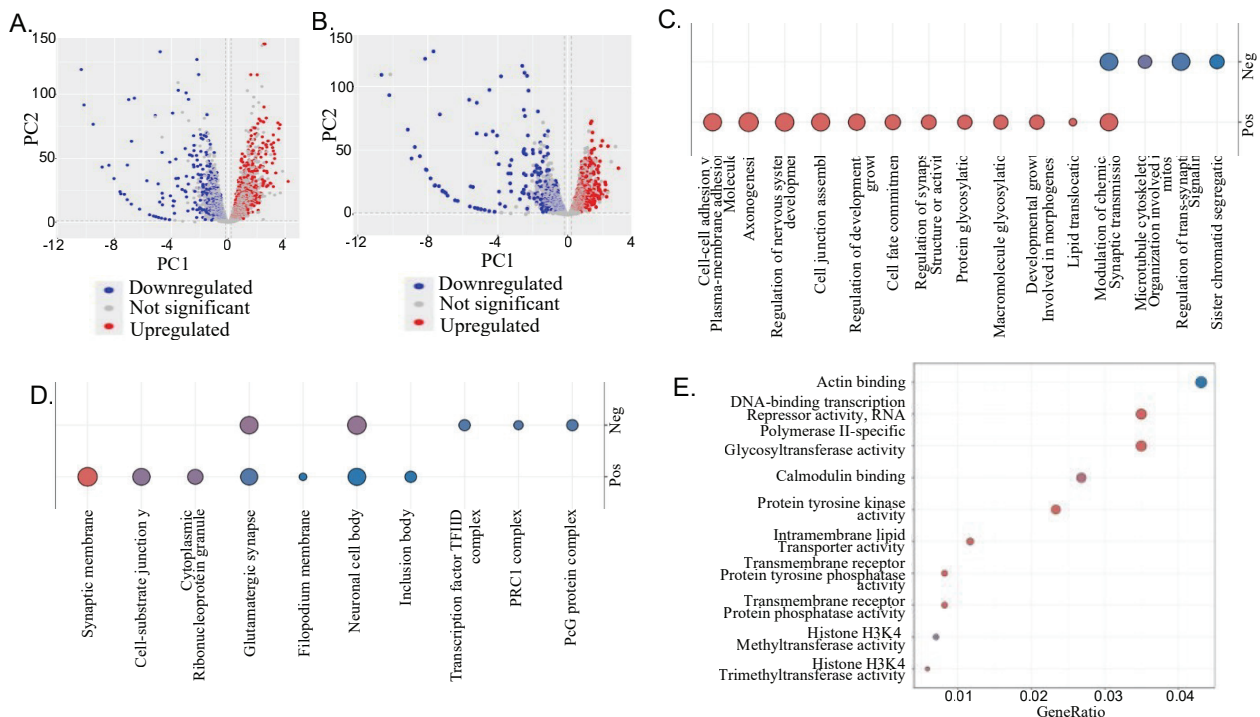


Figure 4. Shared DEGs and enriched pathways in wTDP vs Neg CTRL and cTDP vs Neg CTRL. (A) Volcano plot of wTDP vs. Neg CTRL showing the shared DEGs. (B) Volcano plot of cTDP vs. Neg CTRL showing the shared DEGs. (C-E) Enriched pathways (BP, CC, and MF) based on GO analysis of the shared DEGs in the comparisons of Neg CTRL and wTDP (C), and Neg CTRL and cTDP(D).

demonstrated that ATXN2 loss reversed or attenuated many wTDP-43-induced transcriptomic changes (Figure 5B–D), consistent with its reported neuroprotective role in ALS. Similarly, a comparison between cTDP-AKO and cTDP revealed 3,024 up- and 2,838 down-regulated DEGs (Table 2, Figure 6A). GO enrichment results indicated broad modulation of ALS-relevant molecular pathways (Figure 6B–D). These findings suggest that ATXN2 depletion mitigates cTDP-driven pathogenic transcriptional programs.

Shared DEGs between wTDP-AKO and cTDP-AKO

Cross-comparison of wTDP-AKO vs. wTDP and cTDP-AKO vs. cTDP revealed 1,043 commonly upregulated and 871 commonly downregulated DEGs

(Table 2, Figure 7A–B). Additionally, GO enrichment analyses identified common neuroprotective pathways involved in the beneficial effects of ATXN2 knockout on both nuclear and cytoplasmic TDP-43 variants. These pathways include synapse related pathways, axonogenesis, vesicle/secretory granules, sensory system development, regulation of nervous system development, regulation of nervous system process, developmental growth involved in morphogenesis, developmental induction, establishment/maintenance of cell polarity, tissue migration, response to metal ion, cyclic purine nucleotide metabolic process, dopamine metabolic process, macrophage differentiation, positive regulation of macrophage cytokine production, negative chemotaxis, and regulation of tube size (Figure 7C–D).

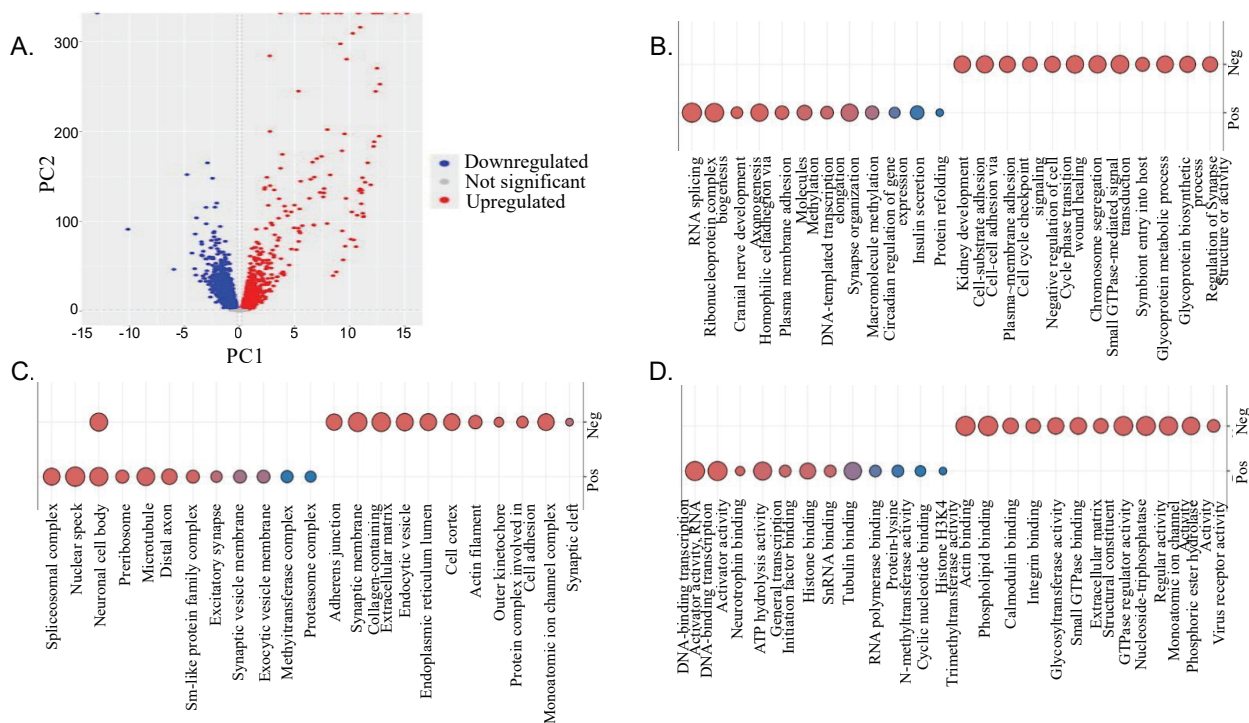


Figure 5. DEGs in wTDP-AKO treatment vs. wTDP groups and their enriched pathways. (A) Volcano plot of the DEGs. (B-D) Enriched pathways (BP, CC, and MF) based on GO analysis of DEGs.

Table 2. The numbers of DEGs in wTDP and cTDP AKO compared with their controls.

Gene Counts	Comparing	wTDP AKO VS wTDP	cTDP AKO VS cTDP	Shared DEGS
Up-regulated Gene Counts		2794	3024	1043
Down-regulated Gene Counts		2956	2838	871

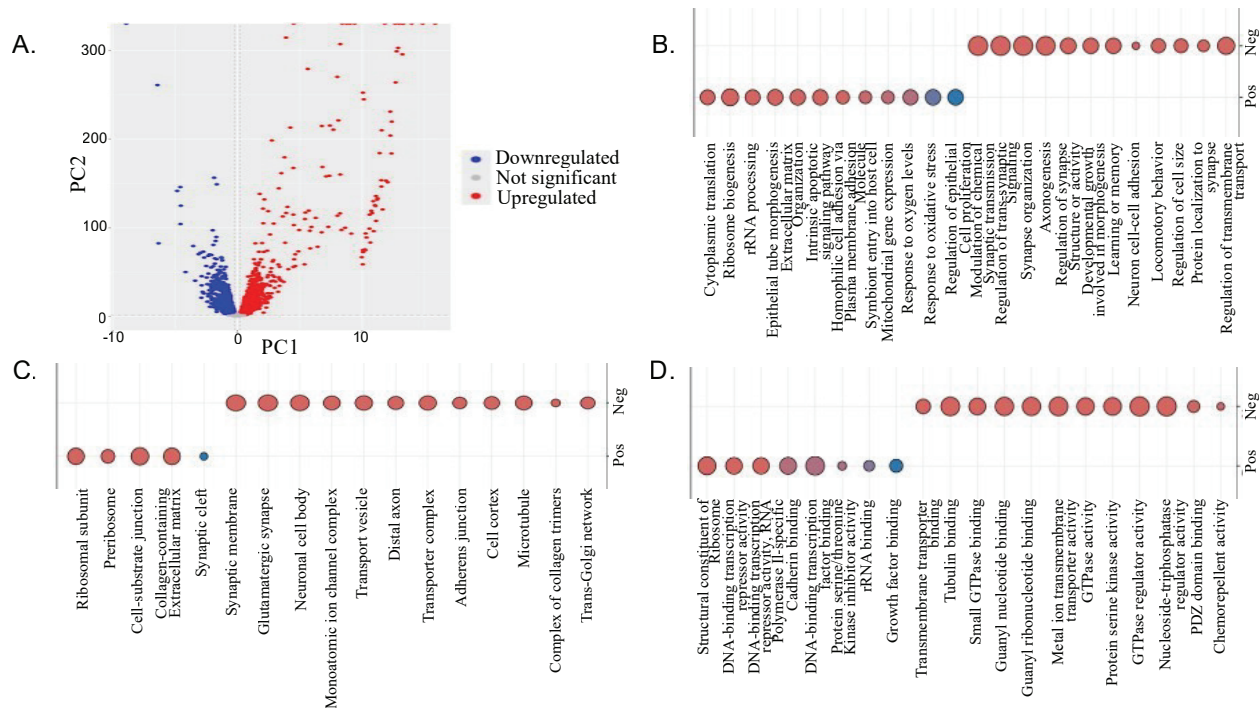


Figure 6. DEGs in *cTDP-AKO* treatment vs. *cTDP* groups and their enriched pathways. (A) Volcano plot of the DEGs. (B-D) Enriched pathways (BP, CC, and MF) based on GO analysis of DEGs.

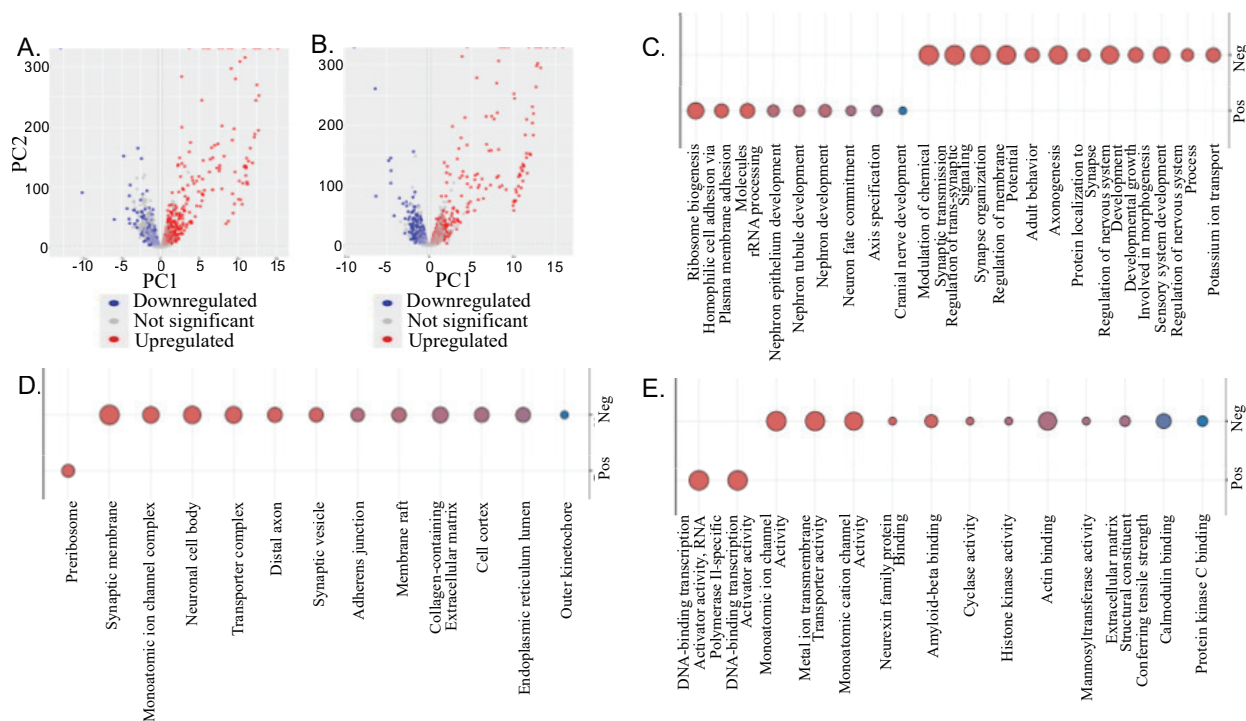


Figure 7. Shared DEGs and enriched pathways between *wTDP-AKO* vs. *wTDP* and *cTDP-AKO* vs. *cTDP*. (A-B) Volcano plot of the shared DEGs in *wTDP-AKO* vs *wTDP* (A) or in *cTDP-AKO* vs *cTDP* (B). (C-E) Enriched pathways (BP, CC, and MF) of the shared DEGs in *wTDP-AKO* vs *wTDP* (C) or in *cTDP-AKO* vs *cTDP* (D).

Integration of Core ALS-Related Gene Signatures

Integrating shared DEGs across TDP-43 variants and ATXN2 rescues on TDP-43 variants identified a core set of 125 pathogenic and 222 protective genes (Table 3). Heatmaps showed the expression difference within these comparison groups (Figure 8 A-B). These genes, along with the enriched BP, CC, and MF pathways revealed by GO analysis (Figure 8 C-E), represent a refined molecular signature genes to ALS pathogenesis and its attenuation via ATXN2 depletion.

Based on the list of pathogenic genes, enriched BP processes included synapse organization, regulation

of trans-synaptic signaling, modulation of chemical synaptic transmission, and cell-cell adhesion via plasma-membrane adhesion molecules, indicating a dysregulation of synaptic signaling and neuronal communication. Enriched CC process included synaptic membrane, glutamatergic synapse, neuron projection terminus, and dense core granule, indicating localization to synaptic compartments and disruption of excitatory neurotransmission. No MF processes were significantly enriched.

Based on the list of protective genes, enriched MF processes included ubiquitin-like protein ligase activity,

Table 3. The shared gene signatures across TDP-43 variants and ATXN2 rescues on TDP-43 variants.

Gene Counts	Comparing	Neg CTRL VS wTDP/cTDP	TDP/cTDP AKO VS wTDP/cTDP	Shared DEGS
Up-regulated Gene Counts		964	871	125
Down-regulated Gene Counts		822	1043	222

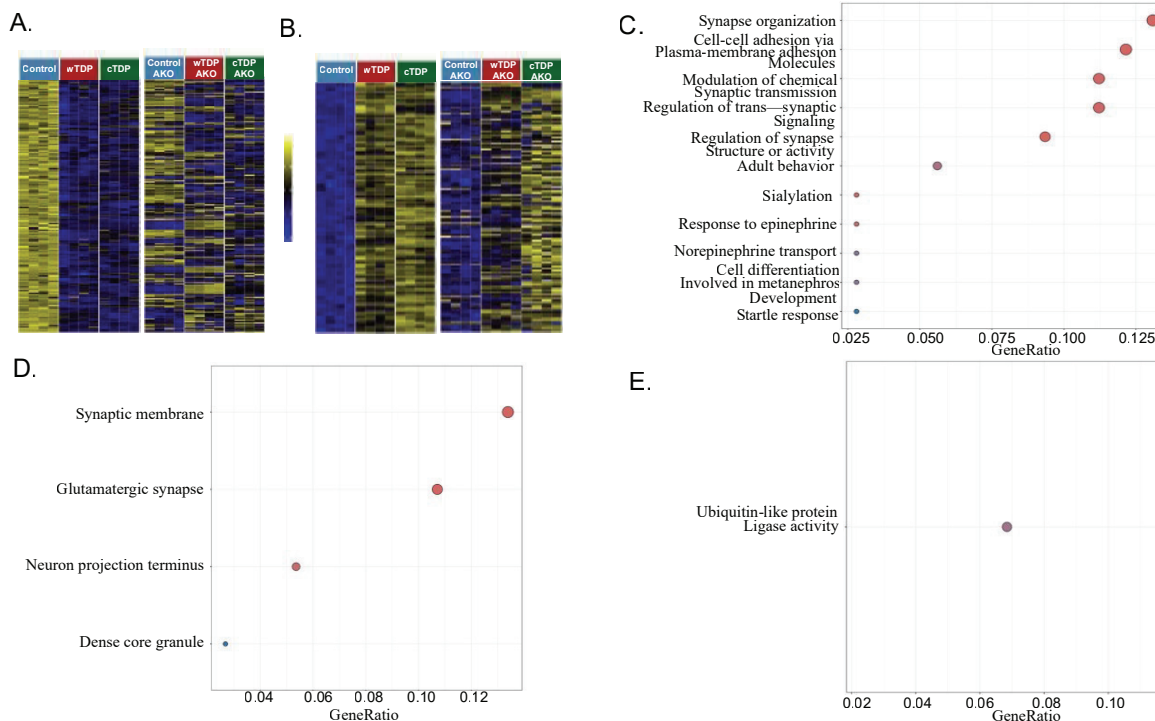


Figure 8. Integration of core ALS-related signature Genes. (A) Heatmaps of the shared down-regulated genes in wTDP or cTDP vs Neg CTRL comparisons and up-regulated genes in wTDP-AKO or cTDP-AKO vs wTDP or cTDP comparisons. (B) Heatmaps of the shared up-regulated genes in wTDP or cTDP vs Neg CTRL comparisons and the down-regulated genes in wTDP-AKO or cTDP-AKO vs wTDP or cTDP comparisons. (C-E) Enriched pathways (BP, CC, and MF) based on GO analysis of the shared DEGs.

indicating that these protective genes may promote tagging and degeneration of misfolded or aggregated proteins, and therefore consistent with a proteostasis-based mechanism of neuroprotection. No BP or CC pathways were significantly enriched.

DISCUSSION

This study demonstrates that both nuclear overexpression and cytoplasmic mislocalization of TDP-43 induce widespread but partially overlapping transcriptomic perturbations in human iPSC-derived motor neuron cultures. Although these two conditions differ in subcellular localization and presumed upstream mechanisms, they converge on a shared downstream transcriptional program. These findings support the idea that TDP-43 pathology in ALS ultimately disrupts common cellular pathways regardless of its nuclear or cytoplasmic origin. Furthermore, CRISPR-mediated knockout of ataxin-2 (ATXN2) broadly attenuated these transcriptomic changes in motor neurons with nuclear overexpression and cytoplasmic mislocalization of TDP-43. Shared DEGs between these comparisons define a core ALS-relevant signature comprising pathogenic and protective genes. Pathway enrichment analysis revealed that pathogenic genes were predominantly involved in synaptic signaling and neuronal communication, whereas protective genes were associated with ubiquitin-like protein ligase activity.

More than individual DEG counts, the key insight from the differential expression analyses lies in the convergence of affected biological processes. Data from the DEG analyses in this study support the aforementioned PCA observations. Over 3,222 genes were upregulated and over 3,302 were downregulated in wTDP vs. Neg CTRL, while cTDP vs. Neg CTRL resulted in 2828 up- and 2949 down-regulated DEGs. The large number of DEGs observed in both comparisons demonstrate the broad impact of TDP-43 dysregulation on transcriptomic gene expression in iPSC-derived human motor neurons (5, 16). This suggests the global regulatory role of TDP-43 in RNA metabolism and gene expression, as well as reflects the use of bulk RNA-seq, which captures averaged transcriptional changes across heterogeneous cell populations. Many biologically relevant regulatory and stress-response genes are expected to exhibit modest effect sizes in bulk RNA-seq datasets, particularly when transcriptional changes occur in subsets of cells or reflect network-level regulation rather than single-gene outputs (17). The shared DEGs

between wTDP and cTDP comparisons, comprising 964 upregulated and 820 downregulated genes, represents a core TDP-43-driven transcriptional signature in ALS motor neurons. This signature includes genes involved in stress granule dynamics, nucleocytoplasmic transport, axonal cytoskeleton maintenance, and autophagy. Many of these pathways have been previously implicated in ALS, such as nucleoporin complex remodeling, reduced expression of axonal transport proteins (e.g., kinesins), and dysregulation of protein degradation pathways (10-12). Importantly, the emergence of these shared DEGs despite differences in subcellular localization of TDP-43 support the hypothesis that TDP-43 pathology in ALS converges on a common set of downstream genes regardless of its nuclear or cytoplasmic origin.

The roles of ATXN2 and TDP-43 in ALS pathogenesis are closely linked. Upregulation of ATXN2 increases TDP-43 toxicity, which has been well established in different models (13,14,18). The present study extends these findings into human iPSC-derived motor neurons. In both wTDP and cTDP conditions, ATXN2 knockout resulted in broad transcriptomic changes that reversed the direction of wTDP or cTDP-induced dysregulation. These data suggest that ATXN2 reinforces ALS pathogenic transcriptional states, and that its depletion alleviates stress on critical cellular processes. The shared DEGs between wTDP-AKO vs. wTDP and cTDP-AKO vs. cTDP likely represent a set of neuroprotective or pathogenic effectors activated or repressed upon ATXN2 loss. Examples of genes with pathogenic associations include ACSL4, KCNJ10, and CHI3L2, which are linked to ferroptosis, excitotoxic vulnerability, and neuroinflammatory responses, respectively. Examples of protective genes include AIFM2, a key ferroptosis suppressor, and HSPA1B, an inducible Hsp70 chaperone that enhances proteostasis and has demonstrated neuroprotection in ALS models (19, 20). Some DEGs are mapped to pathways involved in synaptic vesicle cycling, actin cytoskeleton remodeling, and stress granule disassembly. Given the known role of ATXN2 in RNA granule assembly, these findings are consistent with the hypothesis that ATXN2 depletion prevents persistent stress granule accumulation, which is a feature frequently observed in ALS and other TDP-43 proteinopathies (12).

By integrating genes commonly dysregulated by TDP-43 with those consistently restored by ATXN2 knockout, this study defines a refined core transcriptional signature downstream of the ATXN2-TDP-43 axis. This refined signature potentially defines a biomarker panel for monitoring ALS progression and therapeutic response

to ATXN2-TDP43 targeted interventions. Furthermore, some genes in this panel have been previously implicated in ALS, and the current results provided additional support for their role in ALS (24,25)

Of note, the data analysis supports ATXN2 as a promising target for disease-modifying interventions in ALS. Antisense oligonucleotide-mediated knockdown of ATXN2 has already entered preclinical development, with reports of reduced TDP-43 aggregation and improved survival in mouse models (13,18). The transcriptomic profiles described in the current study provide mechanistic insight into how ATXN2 suppression may exert beneficial effects across distinct forms of TDP-43 pathology. At the same time, ATXN2 is ubiquitously expressed and participates in fundamental RNA regulatory processes. This raises the possibility that systemic modulation may produce off-target effects in non-neuronal tissues. These considerations suggest the potential value of cell-type-specific or context-dependent therapeutic strategies.

While this study provides valuable insights into pathogenic or protective gene expression profiles in different iPSC-derived motor neuron models, it has several limitations. First, iPSC-derived motor neurons represent a valuable and low-cost *in vitro* system for studying ALS disease mechanisms and screen potential therapeutics, but this model can only serve as an initial platform, and *in vivo* validation remains essential. Second, bulk RNA-seq captures culture-level transcriptional changes and does not provide cell-type-resolved resolution or fully disentangle contributions from any remaining co-differentiated populations. Accordingly, the observed differential expression patterns should be interpreted as culture-level effects rather than motor neuron-exclusive changes. Future single-cell RNA-seq (scRNA-seq) study, particularly those based on *in vivo* models, will be necessary to uncover cell type-specific responses to TDP-43 toxicity and ATXN2 depletion. Third, functional validation of candidate genes in the core list and the pathways identified will be required to confirm novel biomarkers and assess any causal role in ALS pathogenesis or neuroprotection.

In conclusion, nuclear and cytoplasmic TDP-43 perturbations converge on overlapping ALS-relevant transcriptional pathways, while ATXN2 knockout broadly restores transcriptomic homeostasis in human iPSC-derived motor neuron cultures. The refined core gene signature identified here provides both mechanistic insight and translational value, which support ATXN2 as a promising disease-modifying target in ALS.

CONCLUSION

Nuclear overexpression and cytoplasmic mislocalization of TDP-43 each disrupt extensive neuronal pathways but converge on a shared ALS-associated transcriptomic signature in human iPSC-derived motor neuron cultures. CRISPR-mediated ATXN2 knockout broadly attenuates these TDP-43-induced transcriptional alterations, thereby restoring key aspects of transcriptomic homeostasis across both nuclear and cytoplasmic contexts. The identification of pathogenic and protective gene signatures downstream of the ATXN2-TDP-43 axis provides new molecular insight into ALS pathogenesis and supports ATXN2 as a promising therapeutic target. Together, these findings refine candidate biomarker panels for ALS and establish a framework for the development of targeted therapeutic strategies.

ACKNOWLEDGEMENTS

I express my gratitude to my mentor, Dr. Qian Wang, for her invaluable guidance and detailed feedback throughout the process of this research project. Her dedication to research has additionally inspired me to persevere in this research project.

FUNDING SOURCES

There are no funding sources to declare.

CONFLICT OF INTEREST

The author declares no conflicts of interest related to this work.

REFERENCES

1. Mead Richard J., Shan Ning, Reiser H. Joseph, *et al*: a neurodegenerative disorder poised for successful therapeutic translation. *Nature Reviews Drug Discovery*. 2023; 22 (3): 185-212. doi:10.1038/s41573-022-00612-2
2. Kiernan Matthew C, Vucic Steve, Cheah Benjamin C, *et al* C. Amyotrophic lateral sclerosis. *The Lancet*. 2011; 377 (9769): 942–955. doi: 10.1016/S0140-6736(10)61156-7
3. Chiò Adriano, Logroscino Giancarlo, Hardiman Orla, *et al*. Prognostic factors in ALS: A critical review. *Amyotrophic Lateral Sclerosis*. 2009; 10 (5-6): 310-323. doi: 10.3109/17482960802566824
4. Lu Lijun, Deng Youqing, Xu Renshi. Current potential

- therapeutics of amyotrophic lateral sclerosis. *Front. Neurol.* 2024; 15. doi:10.3389/fneur.2024.1402962
5. Zarei Sara, Carr Karen, Reiley Luz, *et al.* A comprehensive review of amyotrophic lateral sclerosis. *Surg Neurol Int.* 2015; 6: 171. doi:10.4103/2152-7806.169561
 6. Neumann Manuela, Sampathu Deepak M., Kwong Linda K., *et al.* Ubiquitinated TDP-43 in frontotemporal lobar degeneration and amyotrophic lateral sclerosis. *Science.* 2006; 314 (5796): 130-133. doi:10.1126/science.1134108.
 7. Wang Wenzhang, Wang Luwen, Lu Junjie, *et al.* The inhibition of TDP-43 mitochondrial localization blocks its neuronal toxicity. *Nature Medicine.* doi:10.1038/nm.4130
 8. Al-Chalabi Ammar, Hardiman Orla. The epidemiology of ALS: A conspiracy of genes, environment and time. *Nat Rev Neurol.* 2013 Nov; 9 (11): 617-28. doi:10.1038/nrneurol.2013.203
 9. Limanaqi Fiona, Biagioni Francesca, Gambardella Stefano, *et al.* Promiscuous Roles of Autophagy and Proteasome in Neurodegenerative Proteinopathies. *Proteotoxicity and Neurodegenerative Diseases.* 2020; 21 (8): 3028. doi: 10.3390/ijms21083028
 10. Wu Lien-Szu, Cheng Wei-Cheng, Shen C-K. James. Targeted depletion of TDP-43 expression in the spinal cord motor neurons leads to the development of amyotrophic lateral sclerosis-like phenotypes in mice. *J Biol Chem.* 2012; 287 (36): 30752–30759. doi:10.1074/jbc.M112.359000.
 11. Lee Teresa, Li Yun R., Ingre Caroline, *et al.* Ataxin-2 intermediate-length polyglutamine expansions in European ALS patients. *Hum Mol Genet.* 2011; 20 (9): 1697-1700. doi:10.1093/hmg/ddr045
 12. Elden Andrew C., Kim Hyung-Jun, Hart Michael P, *et al.* Ataxin-2 intermediate-length polyglutamine expansions are associated with increased risk for ALS. *Nature.* 2010; 466 (7310): 1069–1075. doi:10.1038/nature09320
 13. Boulting Gabriella L, Kiskinis Evangelos, Croft Gist F, *et al.* A functionally characterized test set of human induced pluripotent stem cells. *Nat Biotechnol.* 2011; 29 (3): 279–286. doi:10.1038/nbt.1783.
 14. Gill S, Holton KM, Eggan K, Rubin LL. National Center for Biotechnology Information. Gene Expression Omnibus (GEO) accession GSE261875. Available from: <https://www.ncbi.nlm.nih.gov/geo/query/acc.cgi?acc=GSE261875>.
 15. Limone Francesco, San Juan Irune Guerra, Mitchell Jana, *et al.* Efficient generation of lower induced motor neurons by coupling Ngn2 expression with developmental cues. *Cell Rep.* 2023; 42 (1): 111896, doi: 10.1016/j.celrep.2022.111896
 16. Mehta Paul, Raymond Jaime, Zhang Yuze, *et al.* Prevalence of amyotrophic lateral sclerosis in United States, 2018. *Amyotroph Lateral Scler Frontotemporal Degener.* 2023; 24 (6–7): 456–463. doi:10.1080/21678421.2023.2245858.
 17. Liu Yusha, Carbonetto Peter, Willwerscheid Jason, *et al.*, Dissecting tumor transcriptional heterogeneity from single-cell RNA-seq data by generalized binary covariance decomposition. *Nature Reviews Genetics.* 2015: 57 (1): 263-273. doi: 10.1038/s41588-024-01997-z.
 18. Hart Michael P, Gitler Aaron D. ALS-associated ataxin 2 polyQ expansions enhance stress-induced caspase 3 activation and increase TDP-43 pathological modifications. *J Neurosci.* 2012; 32 (27): 9133-42. doi:10.1523/JNEUROSCI.0996-12.2012
 19. Jia Bowen, Li Jing, Song Yiting *et al.*, ACSL4-Mediated Ferroptosis and Its Potential Role in Central Nervous System Diseases and Injuries. *Int. J. Mol. Sci.* 2023; 24 (12): 10021, doi:10.3390/ijms241210021
 20. Kaiser Melanie, Maletzki Iris, Hulsmann Swen, *et al.*, Progressive loss of a glial potassium channel (KCNJ10) in the spinal cord of the SOD1 (G93A) transgenic mouse model of amyotrophic lateral sclerosis. *J Neurochem.* 2006; 99 (3): 900-12. doi: 10.1111/j.1471-4159.2006.04131.x.
 21. Canet-Pons Júlia, Sen Nesli-Ece, Arsović Aleksandar, *et al.* Atxn2-CAG100-KnockIn mouse spinal cord shows progressive TDP43 pathology associated with cholesterol biosynthesis suppression. *Neurobiology of Disease.* 2021; 152. doi.org/10.1016/j.nbd.2021.105289
 22. Vieira de Sá Renata, Sudria-Lopez Emma, Cañizares Luna Marta, *et al.* ATAXIN-2 intermediate-length polyglutamine expansions elicit ALS-associated metabolic and immune phenotypes. *Nature communications.* 2024; 15 (7484). doi.org/10.1038/s41467-024-51676-0
 23. Scoles Daniel R, Gandelman Mandi, Paul Sharan, *et al.* A quantitative high-throughput screen identifies compounds that lower expression of the SCA2- and ALS-associated gene ATXN2. *Journal of biological chemistry.* 2022; 298 (8). doi: 10.1016/j.jbc.2022.102228
 24. Watanabe Ryohei, Higashi Shinji, Nonaka Takashi, *et al.* Intracellular dynamics of Ataxin-2 in the human brains with normal and frontotemporal lobar degeneration with TDP-43 inclusions. *Acta Neuropathologica Communications.* 2020; 8 (176). doi:10.1186/s40478-020-01055-9
 25. Tian Juan, Heinsinger Nicolette, Hu Yinghui, Lim U-Ming, *et al.* Deciphering the interactome of Ataxin-2 and TDP-43 in iPSC-derived neurons for potential ALS targets. *Journals Plos.* 2024. doi:10.1371/journal.pone.0308428